Technische Universität Chemnitz

Sonderforschungsbereich 393

Numerische Simulation auf massiv parallelen Rechnern

Gerd Kunert

Anisotropic mesh construction and error estimation in the finite element method

Preprint SFB393/00-01

Abstract

In an anisotropic adaptive finite element algorithm one usually needs an error estimator that yields the error size but also the stretching directions and stretching ratios of the elements of a (quasi) optimal anisotropic mesh. However the last two ingredients can not be extracted from any of the known anisotropic *a posteriori* error estimators. Therefore a heuristic approach is pursued here, namely, the desired information is provided by the so–called Hessian strategy. This strategy produces favourable anisotropic meshes which result in a small discretization error.

The focus of this paper is on error estimation on anisotropic meshes. It is known that such error estimation is reliable and efficient only if the anisotropic mesh is aligned with the anisotropic solution.

The main result here is that the Hessian strategy produces anisotropic meshes that show the required alignment with the anisotropic solution. The corresponding inequalities are proven, and the underlying heuristic assumptions are given in a stringent yet general form. Hence the analysis provides further inside into a particular aspect of anisotropic error estimation.

Keywords: adaptive algorithm, finite element, anisotropic mesh, anisotropic function, error estimation, Hessian

AMS (MOS): 65N15, 65N30

Preprint-Reihe des Chemnitzer SFB 393

SFB393/00-01 **January 2000**

Für Thilo, der auf tragische Weise ums Leben kam.

Contents

Author's address:

Gerd Kunert
TU Chemnitz
Fakultät für Mathematik
09107 Chemnitz
Germany

`http://www.tu-chemnitz.de/~gku`
`http://www.tu-chemnitz.de/sfb393/`

1 Introduction

Consider some scalar partial differential equation (PDE) in a bounded, polyhedral domain $\Omega \subset \mathbb{R}^d$, $d = 3$ or $d = 2$. For solving such PDEs, finite element computations are nowadays widespread in numerical simulation. The finite element method (FEM) employs a family $\mathcal{F}$ of triangulations $\mathcal{T}$ which consist of elements T. In the setting here, we consider tetrahedra in the three dimensional (3D) case, and triangles in the two dimensional (2D) case. The exact solution of the PDE is denoted by u; the finite element approximation using piecewise linear ansatz functions is denoted by u_h. Other elements (like rectangles) yield similar results. All considerations (apart from section 5) are valid for the 3D and 2D case. Therefore, in most of the analysis the 3D formulas are given; the 2D counterparts can then be derived easily.

In numerical finite element simulations one commonly wants to apply adaptive algorithms that automatically solve the problem up to a given accuracy. The general structure of such an adaptive algorithm is:

0. Start with an initial mesh $\mathcal{T}_0$.
1. Solve the corresponding discrete system.
2. Compute the local *a posteriori* error estimator for each element T of the mesh.
3. When the estimated global error is small enough then stop.
   Otherwise obtain information for a new, better mesh, namely the element size (as a function over Ω).
4. Based on this information, construct a new mesh or perform a mesh refinement, and re-iterate.

Each of these points has attracted much attention by numerous scientists. Nevertheless it may seem surprising that only recently algorithms have have been proposed that can be proven to *converge*, see [Dör96] and [MNS99]. This convincingly illustrates the difficulties when analysing an adaptive algorithm as a whole. These limitations of the present knowledge should be kept in mind when we discuss a certain variant of an adaptive algorithm below.

The framework of this paper is given by a particular class of problems. Namely we consider PDEs that give rise to solutions with strong directional features. These so–called *anisotropic solutions* show much variation in one space direction but little change in other directions. Typical examples include boundary and interior layers, or edge singularities in 3D domains (cf. section 6 for both cases).

It is easily conceivable that an anisotropic solution can be advantageously approximated by a finite element method that employs a so–called *anisotropic mesh*. That is, such a mesh consists of stretched elements; the *stretching ratio* of the elements (also known as *aspect ratio*) can be very large or even unbounded. Implementational and analytical aspects of anisotropic solutions and meshes are given in more detail e.g. in [BK94, FLR96, KR90, Noc95, PVMZ87, Rac93, RGK93, Sie96, Sim94, VH96, ZW94] or in Kunert [Kun99a] and the literature cited therein.

The main interest here consists in the link between anisotropic solutions/meshes and an adaptive algorithm. An anisotropic adaptive algorithm is now obviously different to the isotropic version. In particular the information extraction of step 3 changes to

3. When the estimated global error is small enough then stop.
   Otherwise obtain information for a new, better mesh. This includes:
   - Detect regions of anisotropic behaviour of the solution.
   - Determine a (quasi) optimal stretching direction and stretching ratio of the finite elements in those regions.
   - Determine the element size.

The remeshing algorithm (step 4) also becomes more difficult. Furthermore the error estimation part (step 2) requires reinvestigation too although this is not immediately evident. The reason is that the common error estimators for isotropic meshes fail, or their proofs are no longer valid since the aspect ratio can be unbounded. We may stress here that very few *a posteriori* error estimators for anisotropic meshes are known that are rigorously analysed and proven [Sie96, Kun99a, Kun99b, KV99, DGP99]. In other papers more or less convincing heuristic arguments are given.

Considering the whole adaptive algorithm, it is a quite natural desire that the error estimation (step 2) should provide all necessary information for step 3, in particular the (quasi) optimal element size, the stretching directions and the stretching ratio. The first information (element sizes) can be easily extracted since it is directly related to the value of the local error estimators. For the stretching directions and the stretching ratio the situation is different. Up to now, no error estimator can provide these information.[1] On the contrary, stretching direction and ratio are usually obtained by heuristic methods and constructions. The most popular approaches are:

- **Hessian strategy:** Approximate the Hessian D^2u and perform a *spectral analysis* (also known as *principal axes transformation*). The eigenvectors tell the stretching directions; the eigenvalues give the aspect ratio. See [CHM95, PVMZ87, RGK93, Sim94, ZW94] for a more detailed description.

- **Level lines:** The *level lines* (or *contour lines*) provide a vivid picture of the anisotropy of the function, and thus of the stretching direction. The numerical realization goes back to Kornhuber and Roitzsch [KR90].

- **Gradient jump:** The *gradient jump* of certain values give some indication in which direction the elements should be stretched, see [BK94, Rac93, Sie96].

[1] In Siebert [Sie96] a local condition occurs which serves as a certain kind of 'direction indicator' (for rectangular elements). By a refined analysis and a slight modification of the error estimator, the local condition can be omitted (whilst preserving all other favourite properties, cf. [Kun99a, Remark 3.6]). Thus, the 'direction indication' is purely due to an insufficient analysis and does not really provide the information desired.

In this work we will shed some light onto the **Hessian strategy**. Based on few heuristic assumptions, this strategy is quite convincing and produces useful anisotropic meshes (or at least the underlying information). Here, however, we do not investigate the quality of the mesh construction but show that *the meshes produced are suitable for anisotropic error estimation*. For a precise understanding we have to quote this anisotropic error estimation first.

In Kunert [Kun99a] several local error estimators have been derived and analysed. Three of them fit into the context of this work:

- the residual error estimator $\eta_{R,T}$ for the Poisson equation $-\Delta u = f$,
- the local problem error estimator $\eta_{D,T}$ for the Poisson equation $-\Delta u = f$,
- the residual error estimator $\eta_{\varepsilon,R,T}$ for a singularly perturbed reaction diffusion model problem $-\varepsilon\Delta u + u = f$, with $\varepsilon \ll 1$.

The error bounds below have been derived and proven in [Kun99a] too.

Lemma 1 *The error is bounded* locally from below *for all* $T \in \mathcal{T}$ *by*

$$\eta_T \lesssim |||u - u_h|||_{\omega_T} + \zeta_T \quad . \tag{1}$$

The error is bounded globally from above *by*

$$|||u - u_h|||_\Omega \lesssim m_1(u - u_h, \mathcal{T}) \cdot \left[\sum_{T\in\mathcal{T}} \eta_T^2 + \sum_{T\in\mathcal{T}} \zeta_T^2\right]^{1/2} \quad . \tag{2}$$

The meaning of the terms is as follows:

- The term η_T is one of the aforementioned local error estimators $\eta_{R,T}$, $\eta_{D,T}$ or $\eta_{\varepsilon,R,T}$.
- The norms $|||u - u_h|||_\Omega$ or $|||u - u_h|||_{\omega_T}$ denote the energy norm over the whole domain Ω or the domain ω_T, respectively, where ω_T consists of the element (tetrahedron) T and its (generally) four face neighbours.
- The factor $m_1(u - u_h, \mathcal{T})$ is the so–called *matching function*; its presence is due to the anisotropic mesh. Its precise definition is given in the next section whereas explanatory remarks can be found below.
- The term ζ_T is related to some data approximation. Generally its influence is neglectable; hence this term is not investigated here.
- The notation $x \lesssim y$ or $x \sim y$ is a shorthand for $x \le c \cdot y$ or $c_1 x \le y \le c_2 x$, respectively (with constants independent of x, y, and $\mathcal{T}$).

We may stress here that our analysis is quite general: it relates to all those error estimators and all PDEs that allow an upper error bound (2) containing a factor $m_1(u - u_h, \mathcal{T})$.

In our work here we are not primarily interested (and do not require) the details and the methodology of anisotropic error estimation; for that purpose [Kun99a] and the citations therein are much better sources. Instead, we focus on the matching function $m_1(u - u_h, \mathcal{T})$

which will be defined in the next section. Roughly speaking, the matching function will be $m_1 \sim 1$ for isotropic meshes as well as for anisotropic meshes which are suitably aligned with the anisotropic solution. For inappropriate anisotropic meshes m_1 can be large or even unbounded [Kun99a]. Hence the matching function heavily influences the quality of the upper bound (2).

Up to now, the matching function has been necessary to describe the anisotropic error estimators of [Kun99a] properly. Yet this matching function seemed somewhat exotic, partly because it does not occur in isotropic error estimation[2]. This paper now increases the understanding of the matching function by showing that there are strong links to the Hessian strategy.

Let us now consider the relation between the anisotropic solution and the anisotropic mesh in more detail. Apparently, all anisotropic error estimators require that the anisotropic mesh corresponds in some way with the anisotropic function. Heuristically, one would stretch an element in that direction where the anisotropic function (or, more precisely, its derivative) shows little change. Mathematically, Siebert [Sie96] restricts the set of treatable anisotropic functions, and Kunert [Kun99a, Kun99b] introduces the matching function $m_1(v, \mathcal{T})$ that measures the correspondence between an anisotropic function v and an anisotropic mesh $\mathcal{T}$. Lastly, in [DGP99] a saturation assumption is necessary that implies a similar correspondence.

Despite these different descriptions, the known results strongly indicate that an anisotropic mesh has to correspond to the anisotropic function in order to obtain reliable and efficient error bounds. In the context of the error estimate (2) this means that the matching function is really necessary there (i.e. it is not due to an insufficient analysis).

We remark that the matching function $m_1(u - u_h, \mathcal{T})$ involves the unknown error $u - u_h$. Therefore it can not be computed exactly, but it can be approximated sufficiently well, cf. [Kun99a, Kun99b].

From the definition of m_1 in the next section it follows that always $m_1 > 1$. Lemma 1 on the other hand implies that $m_1(u - u_h, \mathcal{T}) \lesssim 1$ is necessary (with a small c) to obtain tight upper and lower error bounds, and thus reliability and efficiency of the error estimation. Now we can formulate our main result:

> *With only few heuristic assumptions we show that a mesh constructed via the Hessian strategy implies a small matching function, i.e.* $m_1(u - u_h, \mathcal{T}) \lesssim 1$.

As a side effect we strive to put the heuristic assumptions into a stringent mathematical formulation to provide the basis for further analysis (even if this is not possible yet).

At this point a brief summary may additionally improve the understanding. Originally, the Hessian strategy has been developed to produce anisotropic meshes (or, equivalently, the underlying information). Here, however, we show that the Hessian strategy also implies that the matching function $m_1(u - u_h, \mathcal{T})$ is bounded, thus providing tight upper and

[2] More precisely, $m_1 \sim 1$ there, and it merges with other constants.

lower error bounds. Simultaneously, the matching function is a useful tool to assess the (anisotropic) mesh quality.

The remainder of the paper is organized as follows. In section 2 some notation is introduced. The Hessian strategy is presented in section 3. In section 4 it is shown that the Hessian strategy implies a bounded $m_1(u-u_h, \mathcal{T})$. The opposite way we go in section 5: it is shown (in the 2D case) that the Hessian strategy is also a consequence of a bounded matching function m_1. The differences of both results are depicted in the table below:

Section 4: 2D and 3D case. Few heuristic assumptions.	Hessian strategy	$\Rightarrow$	$m_1(u-u_h, \mathcal{T}) \lesssim 1$
Section 5: 2D case only. More heuristic assumptions.	$m_1(u-u_h, \mathcal{T}) \lesssim 1$	$\Rightarrow$	Hessian strategy

This slightly confusing situation is caused by the fact that originally one wants to obtain the result of section 5. This, however, can only be achieved under rather severe heuristic assumptions. With less assumptions and in a mathematically rigerous manner the result of section 4 is derived. This result is not as far–reaching as that of section 5 but still an important improvement.

Finally, some numerical experiments and the summary finish off this paper in sections 6 and 7.

2 Notation

In the following, let $\mathbb{P}^k(\omega)$ be the space of polynomials of order k or less over some domain $\omega \subset \mathbb{R}^d$. The L_2 norm of a function over a domain ω is denoted by $\|\cdot\|_\omega$, and for $\omega = \Omega$ the subscript is omitted. Let $|T|$ be understood as $\mathrm{meas}_d(T)$. With $H^k(\omega)$ we denote the standard Sobolev space of functions whose k–th derivative is in $L_2(\omega)$. This space is equipped with the usual norm.

Let us start with the description of the 3D case. For an arbitrary tetrahedron $T \in \mathcal{T}$, its four vertices are denoted by P_0, P_1, P_2, P_3 such that P_0P_1 is the longest edge of T, $\mathrm{meas}_2(\triangle P_0P_1P_2) \geq \mathrm{meas}_2(\triangle P_0P_1P_3)$, and $\mathrm{meas}_1(P_1P_2) \geq \mathrm{meas}_1(P_0P_2)$. To describe the tetrahedron appropriately we define characteristic *directions* and *lengths*.

- The *directions* are indicated by three pairwise orthonormal vectors $\mathbf{p}_{i,T}$, cf. figure 1. Since we are only interested in the directions, the vectors $\mathbf{p}_{i,T}$ shall be scaled such that $|\mathbf{p}_{i,T}| = 1$. When unambiguous, the subscript T is omitted.

- The *lengths* are the dimensions of T along the directions $\mathbf{p}_{i,T}$, i.e.
  $$h_{1,T} := \mathrm{meas}_1(P_0P_1)$$
  $$h_{2,T} := 2\mathrm{meas}_2(\triangle P_0P_1P_2) \,/\, \mathrm{meas}_1(P_0P_1)$$
  $$h_{3,T} := 3\mathrm{meas}_3(T) \,/\, \mathrm{meas}_2(\triangle P_0P_1P_2).$$
  Observe $h_{1,T} > h_{2,T} \geq h_{3,T}$ and set
  $$h_{min,T} := h_{3,T}.$$

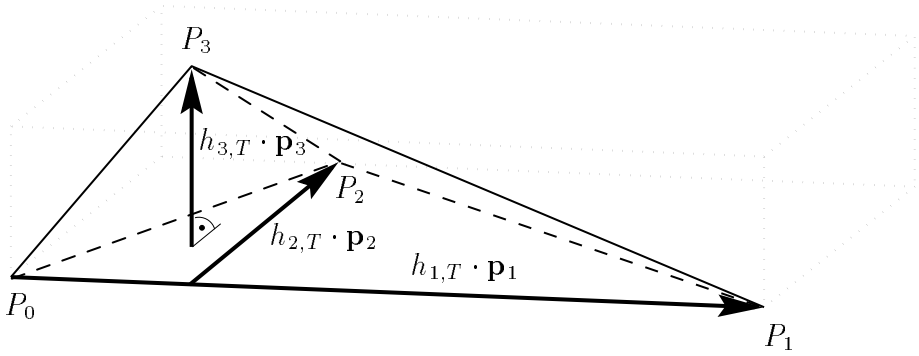

Figure 1: Notation of tetrahedron T

In the 2D case the notation is almost the same. There the triangle has the vertices P_0, P_1, P_2; the directions $\mathbf{p}_{1,T}$, $\mathbf{p}_{2,T}$ and lengths $h_{1,T} > h_{2,T}$ are defined in a similar fashion. Here one sets $h_{min,T} := h_{2,T}$.

In the analysis, derivatives of some functions play an important role. The so–called *Hessian* is the matrix of the second–order derivatives, denoted by

$$D^2 u \;:=\; \left(\partial_{x_i}\partial_{x_j} u\right)_{i,j=1}^{d}$$

where $\partial_{x_i} v$ is the partial first–order derivative.

When analysing the anisotropic error estimates, certain *directional derivatives* can be favourably employed, cf. [Kun99a]. For arbitrary directions (vectors) $\mathbf{l}_1, \mathbf{l}_2$ we thus define the first–order directional derivative by

$$\partial_{\mathbf{l}_1} u \;:=\; |\mathbf{l}_1|^{-1} \cdot \mathbf{l}_1^\top \nabla u \;\equiv\; |\mathbf{l}_1|^{-1} \cdot (\nabla u, \mathbf{l}_1) \;\equiv\; \partial u / \partial \mathbf{l}_1 \qquad ,$$

and the second–order directional derivative by

$$\partial^2_{\mathbf{l}_1\mathbf{l}_2} u \;:=\; |\mathbf{l}_1|^{-1}|\mathbf{l}_2|^{-1} \cdot \mathbf{l}_1^\top D^2 u\, \mathbf{l}_2 \;\equiv\; |\mathbf{l}_1|^{-1}|\mathbf{l}_2|^{-1} \cdot (D^2 u\, \mathbf{l}_1, \mathbf{l}_2) \;\equiv\; \partial^2 u / \partial \mathbf{l}_1 \partial \mathbf{l}_2 \qquad ,$$

where $|\mathbf{l}_i|$ denotes the length of the vector and $(\cdot,\cdot)$ is the usual Euclidean scalar product.

In the Hessian strategy which is described in the next section the Hessian $D^2 u$ naturally is of great importance. However in real applications $D^2 u$ is not known since it involves the exact solution u. Hence a so–called *approximate Hessian*

$$D^{2,h} u_h \;\approx\; D^2 u$$

has to be computed from the known approximate solution u_h. This can be achieved via a recovered gradient, for example. Here we do not discuss this question but assume instead that a symmetric and sufficiently good approximation $D^{2,h} u_h$ is provided. In sections 4.2 and 4.4 we explain what 'sufficiently good' means.

For the approximate Hessian we want to utilize the equivalent of the directional derivatives and therefore define

$$\partial^{2,h}_{\mathbf{l}_1\mathbf{l}_2} u_h \;:=\; |\mathbf{l}_1|^{-1}|\mathbf{l}_2|^{-1} \cdot \mathbf{l}_1^\top D^{2,h} u_h\, \mathbf{l}_2 \;\equiv\; |\mathbf{l}_1|^{-1}|\mathbf{l}_2|^{-1} \cdot (D^{2,h} u_h\, \mathbf{l}_1, \mathbf{l}_2) \qquad .$$

With the help of the directional derivatives we can now present the *matching function*:

$$m_1(v,\mathcal{T}) := \left[\frac{\displaystyle\sum_{T\in\mathcal{T}} \sum_{i=1}^{3} \frac{h_{i,T}^2}{h_{min,T}^2} \cdot \|\partial_{\mathbf{p}_i} v\|_T^2}{\displaystyle\sum_{T\in\mathcal{T}} \sum_{i=1}^{3} \|\partial_{\mathbf{p}_i} v\|_T^2} \right]^{1/2} \tag{3}$$

(recall that $\mathbf{p}_i \equiv \mathbf{p}_{i,T}$ are the directions of the element T). The lower bound $m_1 > 1$ is obvious.

3 The Hessian strategy

The Hessian strategy has been known for quite a long time, see e.g. [CHM95, PVMZ87, RGK93, Sim94, ZW94]. For a given anisotropic function it provides the description of a suitable anisotropic mesh for that function (in terms of stretching direction and ratio of the elements). A simple, heuristically convincing and straight–forward motivation is as follows.

Motivation (2D case): Consider a single triangle T and an arbitrary quadratic function v. Minimize the interpolation error in the H^1 seminorm $\|\nabla(v - \mathrm{I}_L v)\|_T$ over all (right–angled) triangles T with prescribed area $|T|$. Here $\mathrm{I}_L v \in \mathbb{P}^1(T)$ shall be the usual nodal Lagrange interpolate. Compute the (constant) Hessian $D^2 v$, its two real eigenvalues λ_1, λ_2 such that $|\lambda_1| \le |\lambda_2|$, and the corresponding eigenvectors $\mathbf{p}_1$ and $\mathbf{p}_2$. Then the quasi minimal interpolation error (up to some constant factor) is achieved for those triangles that are stretched along $\mathbf{p}_1$, and whose stretching ratio is $\sqrt{|\lambda_2|} : \sqrt{|\lambda_1|} \ge 1$.

To describe the *general* Hessian strategy properly, we formally split it into step 3 of the adaptive algorithm (information extraction) and step 4 (remeshing). This separation allows us to address the assumptions appropriately but also the drawbacks. Our main interest is the information extraction (step 3). Furthermore several remeshing algorithms (step 4) are presented but not discussed in detail. To include all the diverse remeshing methods in our analysis, we will pose one condition that a newly constructed mesh has to satisfy.

Next the Hessian strategy is presented.

Step 3: Information extraction
Although the finite element error $\|\nabla(u - u_h)\|$ should be minimized, one considers instead the simpler interpolation error $\|\nabla(u - \mathrm{I}_L u)\|$ which leads to the Hessian $D^2 u$. Since $D^2 u$ is not known one has to utilize a symmetric approximation $D^{2,h} u_h$ to $D^2 u$. We assume that such an approximation is provided.

The information desired are the stretching directions and the aspect ratio. Generally speaking, they are functions on Ω, and they are given by the eigenvalues and eigenvectors of

$D^{2,h}u_h$. This procedure is known as *spectral decomposition* or *principal axes transformation* of the matrix $D^{2,h}u_h$:

$$\begin{array}{lll} \text{Eigenvectors of } D^{2,h}u_h\text{:} & \mathbf{q}_i(x) & i=1,2,3 \qquad (4)\\ & \text{Assume } |\mathbf{q}_i(x)| = 1. & \end{array}$$

$$\begin{array}{lll} \text{Eigenvalues of } D^{2,h}u_h\text{:} & \mu_i(x) := \lambda_i(D^{2,h}u_h(x)) & i=1,2,3 \qquad (5)\\ & \quad \equiv (D^{2,h}u_h(x)\cdot \mathbf{q}_i(x), \mathbf{q}_i(x)) & \\ & \quad = \partial^{2,h}_{\mathbf{q}_i\,\mathbf{q}_i} u_h(x) & \\ & \text{Assume } |\mu_1(x)| \le |\mu_2(x)| \le |\mu_3(x)|. & \end{array}$$

$$\text{Stretching length:} \qquad H_i(x) := \alpha_{\mathcal{T}} \cdot |\mu_i(x)|^{-1/2} \qquad i=1,2,3 \qquad (6)$$

For each $x \in \Omega$ the stretching directions are $\mathbf{q}_i(x)$, and the stretching lengths are $H_i(x), i = 1,2,3$.

The global parameter $\alpha_{\mathcal{T}}$ is the same for all elements T. For the ease of our exposition, we assume that all $\mu_i(x)$ are distinct, i.e. $|\mu_1(x)| < |\mu_2(x)| < |\mu_3(x)|$. This is, of course, not realistic in real world applications. Then the algorithmic implementation is more sophisticated, and the description has to be changed (for example, by using a set of three vectors $\{H_i(x)\cdot \mathbf{q}_i(x)\}_{i=1}^3$ without any ordering).

Step 4: Remeshing

Once the functions of the stretching directions and stretching lengths are known, the new mesh $\mathcal{T}_{new}$ is to be constructed. We will mention several approaches for the remeshing. In order to treat all of them in our context here, we formulate a rather general condition that has be be satisfied. We note that this condition comprises most of the heuristic assumptions (or, in some sense, the essence of the Hessian strategy), cf. the discussion below.

When a new triangle $T_{new} \in \mathcal{T}_{new}$ is to be constructed[3], its directions $\mathbf{p}_{i,T_{new}}$ and lengths $h_{i,T_{new}}$ should be close to the computed information $\mathbf{q}_i(x), H_i(x)$:

$$\begin{array}{lcll} \mathbf{p}_{i,T_{new}} & \approx & \mathbf{q}_i(x) & \forall\, x \in T_{new} \\ h_{i,T_{new}} & \approx & H_i(x) & \forall\, x \in T_{new} \qquad . \end{array}$$

The 'closeness' could be measured, for example, in some integral sense. It also displays an immediate difficulty: T_{new} should be constructed according to $\mathbf{q}_i(x), H_i(x)$, but these data should be considered for all points $x \in T_{new}$ of the triangle to be constructed. This dependence (depicted by $\longleftarrow$) can be illustrated as follows:

$$T_{new} \quad \longleftarrow \quad \mathbf{p}_{i,T_{new}}, h_{i,T_{new}} \quad \longleftarrow \quad \mathbf{q}_i(x)\Big|_{T_{new}}, H_i(x)\Big|_{T_{new}} \quad \longleftarrow \quad T_{new}$$

This self–dependent (reflexive) description can be dealt with in several ways.

Firstly, one may iteratively construct the new element: Start with an initial guess $T_{new,1}$, determine $\mathbf{q}_i(x)|_{T_{new,1}}, H_i(x)|_{T_{new,1}}$, recompute $\mathbf{p}_{i,T_{new,2}}, h_{i,T_{new,2}}$, and construct an improved guess $T_{new,2}$ until a sufficient correspondence is achieved.

[3]For easier recollection we denote the mesh to be constructed by $\mathcal{T}_{new}$.

A second approach consists of constructing a global transformation such that the transformed domain can be meshed uniformly and isotropically, cf. [Sim94]. However such a transformation does not necessarily exist. Even if it exists, its construction requires solving a system of ordinary differential equations.

A third group of approaches heavily relies on the use of a Riemannian metric tensor; they try to construct equilateral triangles with respect to that metric. For more details or different methods see e.g. [BH96] or [Kun99a] and the citations therein.

Here we will not present and analyse these remeshing algorithms in detail. Yet we want our analysis to include all these constructions, and probably even completely different approaches (e.g. the contour lines approach, cf. section 1). For that reason we pose one rather general assumption: We allow *any* construction of $\mathcal{T}_{new}$ as long as the condition below is satisfied for all tetrahedra $T_{new} \in \mathcal{T}_{new}$:

$$h^2_{i,T_{new}} \cdot \|\partial^2_{\mathbf{p}_i\mathbf{p}_i} u\|_{T_{new}} \;\sim\; \alpha^2_{\mathcal{T}} \cdot |T_{new}|^{1/2} \qquad i = 1,2,3. \tag{7}$$

This condition contains much of the essence of the remeshing part of the Hessian strategy and its heuristic assumptions. The condition and its plausibility are investigated in more detail in section 4.2.

Remark 1 The choice of the parameter $\alpha_{\mathcal{T}}$ is less restrictive as it may seem at first. For example $\alpha_{\mathcal{T}}$ can also be a function $\alpha_{\mathcal{T}}(x)$ as long as it does not change rapidly across adjacent tetrahedra. □

4 On the boundedness of the matching function

In this section we will show that a mesh construction based on the Hessian strategy results in a bounded matching function, i.e. $m_1(u - u_h, \mathcal{T}) \sim 1$. Of course, the Hessian strategy (implicitly) includes certain heuristic assumptions. In order to obtain a rigorous proof, we try to specify, analyse and discuss these assumptions as precise as possible.

In section 4.1 we present local anisotropic *a priori* interpolation error estimates which are central to our analysis. Section 4.2 lists the heuristic assumptions, both as a verbal description and as formulas. The actual proof of a bounded matching function is given in section 4.3, and the heuristic assumptions are discussed in more detail in section 4.4.

4.1 Local interpolation estimates

Local *a priori* interpolation estimates on anisotropic elements are widely developed in the literature. Here we want to use an interpolation operator that

- is suitable for 2D and 3D elements,
- involves preferably only the element T under consideration,
- allows an estimation of first–order partial derivatives against second–order derivatives.

Here we have chosen the *Crouzeix–Raviart* interpolant I_{CR}, cf. [ANS99]. The less suitable *Lagrange* interpolant I_L is presented afterwards.

Crouzeix–Raviart interpolant: This interpolant $\mathrm{I}_{CR} : W^{1,p}(T) \mapsto \mathbb{P}^1(T)$ is defined for all functions $v \in W^{1,p}$, $p \in [1, \infty]$, and it is uniquely defined by the condition

$$\int_F v - \mathrm{I}_{CR} v = 0 \qquad \forall \text{ faces } F \subset \partial T \qquad .$$

Here $W^{1,p}$ denotes the usual Sobolev space. From now on only the case $p = 2$ is required; then $W^{1,p}$ becomes the Hilbert space H^1.

Apel/Nicaise/Schöberl [ANS99, Lemma 3.3] have proven the following lemma.

Lemma 2 *Let $u \in H^2(T)$. Then*

$$\|\partial_{\mathbf{p}_i}(u - \mathrm{I}_{CR} u)\|_T \lesssim \sum_{j=1}^{3} h_{j,T} \cdot \|\partial^2_{\mathbf{p}_i \mathbf{p}_j} u\|_T \qquad i = 1, 2, 3. \tag{8}$$

Note that the additional assumptions of [ANS99, Lemma 3.3] are automatically satisfied here since we utilize the directional derivatives, and the case $p = 2$. Furthermore no maximum angle condition is required.

For completeness we also present a similar result for the Lagrange (i.e. nodal) interpolant I_L. This interpolant can be defined for the 2D and the 3D case. The corresponding interpolation error estimates, however, are valid only in 2D.

Lagrange interpolant: Let $v \in H^2(T) \hookrightarrow C^0(\bar{T})$ for $T \subset \mathbb{R}^d$. Then $\mathrm{I}_L : H^2(T) \mapsto \mathbb{P}^1(T)$ is uniquely defined by the condition

$$(\mathrm{I}_L v)(x) = v(x) \qquad \forall \text{vertices } x \in \bar{T} \qquad .$$

For the 2D case Apel and Dobrowolski [AD92] have shown that

$$\|\partial_{\mathbf{p}_1}(u - \mathrm{I}_L u)\|_T \lesssim h_{1,T} \cdot \|\partial^2_{\mathbf{p}_1 \mathbf{p}_1} u\|_T + h_{2,T} \cdot \|\partial^2_{\mathbf{p}_1 \mathbf{p}_2} u\|_T + \frac{h^2_{2,T}}{h_{1,T}} \cdot \|\partial^2_{\mathbf{p}_2 \mathbf{p}_2} u\|_T \tag{9}$$

$$\|\partial_{\mathbf{p}_2}(u - \mathrm{I}_L u)\|_T \lesssim h_{1,T} \cdot \|\partial^2_{\mathbf{p}_1 \mathbf{p}_1} u\|_T + h_{1,T} \cdot \|\partial^2_{\mathbf{p}_1 \mathbf{p}_2} u\|_T + h_{2,T} \cdot \|\partial^2_{\mathbf{p}_2 \mathbf{p}_2} u\|_T \quad . \tag{10}$$

Note that (10) requires a maximum angle condition.

4.2 The heuristic assumptions

All adaptive algorithms with the Hessian strategy contain certain heuristic assumptions (probably in some disguise) which can be classified roughly as follows.

- the Hessian strategy is feasible,
- sufficiently good approximation of the Hessian: $D^{2,h}u_h \approx D^2u$,
- the Hessian does not change rapidly across adjacent elements,
- the interpolation estimates are sharp enough,
- $u_h \approx \mathrm{I}_{CR}u$ in the sense of the matching function m_1.

These conditions are now reformulated in a strict mathematical form. A detailed discussion also of the shortcomings of these assumptions is given in section 4.4 below.

1. **The Hessian strategy is feasible**
   This implies that the Hessian can be computed, i.e.

   $$u \in H^2(\Omega) \qquad . \tag{A.1}$$

   Furthermore the stretching lengths are defined via $H_i(x) := \alpha_{\mathcal{T}} \cdot |\mu_i(x)|^{-1/2}$, cf. (6). Strictly speaking, this requires $\mu_i(x) \neq 0$. Here, however, we formally allow $\mu_i(x) = 0$ implying $H_i(x) = \infty$. Then the remeshing part of the Hessian strategy has to deal with this 'exception'. The other assumptions below have to hold as well, even if the heuristic reasoning may be less convincing (cf. assumption (A.3) for example).

2. $D^{2,h}u_h \approx D^2u$ **and** D^2u **does not change too much**
   Assume for the moment that the Hessian D^2u is constant (i.e. u is quadratic), and that the directions $\mathbf{p}_{i,T_{new}}$ of the new element are chosen to be the eigenvectors of D^2u (instead of its approximation $D^{2,h}u_h$). The principle of the spectral decomposition of the Hessian D^2u readily implies

   $$\partial^2_{\mathbf{p}_i\mathbf{p}_j}u = 0 \qquad \forall\, i \neq j \qquad .$$

   In reality, however, D^2u is rarely constant, and the directions $\mathbf{p}_{i,T_{new}}$ are computed from $D^{2,h}u_h$. Yet if D^2u does not change too much and if $D^{2,h}u_h \approx D^2u$ then $\partial^2_{\mathbf{p}_i\mathbf{p}_j}u$ should almost vanish. This is expressed by the condition

   $$h_{j,T} \cdot \|\partial^2_{\mathbf{p}_i\mathbf{p}_j}u\|_T \lesssim h_{i,T} \cdot \|\partial^2_{\mathbf{p}_i\mathbf{p}_i}u\|_T \qquad \forall\, i \neq j \qquad . \tag{A.2}$$

   The next assumption has already been mentioned in section 3 when introducing the Hessian strategy:

   $$h^2_{i,T_{new}} \cdot \|\partial^2_{\mathbf{p}_i\mathbf{p}_i}u\|_{T_{new}} \sim \alpha^2_{\mathcal{T}} \cdot |T_{new}|^{1/2} \qquad i = 1,2,3, \quad \forall\, T_{new} \in \mathcal{T}_{new}, \tag{A.3}$$

   with some global parameter $\alpha_{\mathcal{T}}$. This assumption is almost the essence of the remeshing part of the Hessian strategy; it relates the information extracted from the given mesh $\mathcal{T}_{old}$ (i.e. $\mathbf{q}_i(x), H_i(x)$) to the newly constructed mesh $\mathcal{T}_{new}$.

   The plausibility of the assumption is shown in section 4.4.

3. **The interpolation estimates are sharp**
Lemma 2 states that

$$\|\partial_{\mathbf{p}_i}(u - \mathrm{I}_{CR}u)\|_T \lesssim \sum_{j=1}^{3} h_{j,T} \cdot \|\partial^2_{\mathbf{p}_i\mathbf{p}_j} u\|_T \qquad i = 1,2,3.$$

For a strict proof, we require the equivalence (i.e. $\sim$ instead of $\lesssim$), or at least

$$\|\partial_{\mathbf{p}_i}(u - \mathrm{I}_{CR}u)\|_T \gtrsim h_{i,T} \cdot \|\partial^2_{\mathbf{p}_i\mathbf{p}_i} u\|_T \qquad i = 1,2,3 \qquad . \tag{A.4}$$

In section 4.4 this condition is further investigated. Note that (A.4) can be further weakened to

$$\sum_{i=1}^{3} \|\partial_{\mathbf{p}_i}(u - \mathrm{I}_{CR}u)\|_T \gtrsim h_{3,T} \cdot \|\partial^2_{\mathbf{p}_3\mathbf{p}_3} u\|_T \qquad . \tag{A.4'}$$

4. $u_h \approx \mathrm{I}_{CR}u$ **in the sense of the matching function** m_1
To transform this into a formula, we simply require

$$m_1(u - u_h, \mathcal{T}) \sim m_1(u - \mathrm{I}_{CR}u, \mathcal{T}) \tag{A.5}$$

because the right–hand side is much easier to investigate. The numerical experiments of section 6 show that this is a realistic demand.

4.3 Bounding the matching function

Let us first recollect the heuristic assumptions (A.1)–(A.5) which have to be satisfied for all elements $T \equiv T_{new}$ of the newly constructed mesh $\mathcal{T}$.

$$\begin{aligned}
u &\in H^2(\Omega) && && (A.1)\\
h_{j,T} \cdot \|\partial^2_{\mathbf{p}_i\mathbf{p}_j} u\|_T &\lesssim h_{i,T} \cdot \|\partial^2_{\mathbf{p}_i\mathbf{p}_i} u\|_T && \forall\, i \neq j && (A.2)\\
h^2_{i,T} \cdot \|\partial^2_{\mathbf{p}_i\mathbf{p}_i} u\|_T &\sim \alpha^2_{\mathcal{T}} \cdot |T|^{1/2} && i = 1,2,3, \quad \forall\, T \in \mathcal{T} && (A.3)\\
\|\partial_{\mathbf{p}_i}(u - \mathrm{I}_{CR}u)\|_T &\gtrsim h_{i,T} \cdot \|\partial^2_{\mathbf{p}_i\mathbf{p}_i} u\|_T && i = 1,2,3 && (A.4)\\
m_1(u - u_h, \mathcal{T}) &\sim m_1(u - \mathrm{I}_{CR}u, \mathcal{T}) \qquad . && && (A.5)
\end{aligned}$$

The main result is as follows.

Theorem 3 (Bounded matching function) *Assume that (A.1)–(A.5) hold. Then*

$$m_1(u - u_h, \mathcal{T}) \sim 1 \qquad . \tag{11}$$

Proof: We start with the matching function $m_1(u - \mathrm{I}_{CR}u, \mathcal{T})$ for the *interpolation error* which is defined by

$$m_1(u - \mathrm{I}_{CR}u, \mathcal{T}) = \left(\sum_{T \in \mathcal{T}} y_T \Big/ \sum_{T \in \mathcal{T}} z_T \right)^{1/2} , \tag{12}$$

$$\text{with} \qquad y_T := \sum_{i=1}^{3} \frac{h_{i,T}^2}{h_{min,T}^2} \cdot \|\partial_{\mathbf{p}_i}(u - \mathrm{I}_{CR}u)\|_T^2 \tag{13}$$

$$\text{and} \qquad z_T := \sum_{i=1}^{3} \|\partial_{\mathbf{p}_i}(u - \mathrm{I}_{CR}u)\|_T^2 \tag{14}$$

being the element–related terms of the numerator and the denominator, respectively, cf. (3).

With the help of the interpolation error estimate (8) and the assumptions (A.2), (A.3) one derives for the numerator

$$\begin{aligned} y_T &= h_{min,T}^{-2} \sum_{i=1}^{3} h_{i,T}^2 \cdot \|\partial_{\mathbf{p}_i}(u - \mathrm{I}_{CR}u)\|_T^2 \\ &\overset{(8)}{\lesssim} h_{min,T}^{-2} \sum_{i=1}^{3} h_{i,T}^2 \sum_{j=1}^{3} h_{j,T}^2 \cdot \|\partial_{\mathbf{p}_i \mathbf{p}_j}^2 u\|_T^2 \\ &\overset{(A.2)}{\lesssim} h_{min,T}^{-2} \sum_{i=1}^{3} h_{i,T}^4 \cdot \|\partial_{\mathbf{p}_i \mathbf{p}_i}^2 u\|_T^2 \\ &\overset{(A.3)}{\sim} h_{min,T}^{-2} \cdot \alpha_{\mathcal{T}}^4 \cdot |T| \qquad . \end{aligned}$$

Similarly the denominator is investigated.

$$\begin{aligned} z_T &= \sum_{i=1}^{3} \|\partial_{\mathbf{p}_i}(u - \mathrm{I}_{CR}u)\|_T^2 \\ &\overset{(A.4)}{\gtrsim} \sum_{i=1}^{3} h_{i,T}^2 \cdot \|\partial_{\mathbf{p}_i \mathbf{p}_i}^2 u\|_T^2 \equiv \sum_{i=1}^{3} h_{i,T}^{-2} \cdot h_{i,T}^4 \cdot \|\partial_{\mathbf{p}_i \mathbf{p}_i}^2 u\|_T^2 \\ &\overset{(A.3)}{\sim} \alpha_{\mathcal{T}}^4 \cdot |T| \cdot \sum_{i=1}^{3} h_{i,T}^{-2} \qquad . \end{aligned}$$

Hence one readily obtains

$$y_T \lesssim \alpha_{\mathcal{T}}^4 \cdot |T| \cdot h_{min,T}^{-2} \leq \alpha_{\mathcal{T}}^4 \cdot |T| \cdot \sum_{i=1}^{3} h_{i,T}^{-2} \lesssim z_T$$

and

$$\sum_{T \in \mathcal{T}} y_T \lesssim \sum_{T \in \mathcal{T}} z_T \qquad .$$

Together with (A.5) this implies

$$m_1(u-u_h,\mathcal{T}) \overset{(A.5)}{\sim} m_1(u-\mathrm{I}_{CR}u,\mathcal{T}) = \left[\sum_{T\in\mathcal{T}} y_T \Big/ \sum_{T\in\mathcal{T}} z_T\right]^{1/2} \lesssim 1 \quad .$$

Since $1 \le m_1(u-u_h,\mathcal{T})$ is obvious the desired result is proven. ∎

4.4 The assumption revisited – Difficulties of the Hessian strategy

The Hessian strategy is only a heuristic strategy, and as such, it has naturally its limitations. In this section we try to describe and analyse these limits as rigorously as possible. For that it is convenient to distinguish between problems that are due to the Hessian strategy, and problems that are due to the analysis of the method. Not surprisingly there are close connections to the heuristic assumptions (A.1)–(A.5) of section 4.2, see also there for a comparison. So let us recall and discuss these assumptions.

Assumption (A.1): $u \in H^2(\Omega)$

In practical applications the solution is not necessarily as smooth as $H^2(\Omega)$. Even for the Poisson equation in a 3D domain with a concave edge or with changing boundary conditions one generically obtains only $u \in H^{1+\gamma}(\Omega), 0<\gamma<1$.

Then the Hessian strategy may run into difficulties as D^2u and $D^{2,h}u_h$ can be expected to become very large or even unbounded in certain regions. The aspect ratio may tend to $1:\infty$, thus rendering the Hessian strategy infeasible. Furthermore not only the Hessian strategy itself fails but also its analysis, since the interpolation estimates do not hold anymore (e.g. $\partial^2_{\mathbf{p}_i\mathbf{p}_j}u$ may not be defined).

A partial remedy can be seen in the fact that the solution u has regularity H^2 in most of the domain Ω, and that less regularity occurs only in small regions. For example for the 3D Poisson equation with a concave edge, u is singular only along that edge. Therefore the Hessian strategy will probably work well in most of the domain, and only small regions require an additional treatment. This treatment could, for example, consist of a bound that the aspect ratio must not exceed.

Assumption (A.2): $h_{j,T}\cdot\|\partial^2_{\mathbf{p}_i\mathbf{p}_j}u\|_T \lesssim h_{i,T}\cdot\|\partial^2_{\mathbf{p}_i\mathbf{p}_i}u\|_T \qquad \forall\, i\neq j$

In the imaginary, 'ideal' case of $D^2u = D^{2,h}u_h = const$ and $\mathbf{p}_{i,T} = \mathbf{q}_i(x)$ the mixed derivatives $\partial^2_{\mathbf{p}_i\mathbf{p}_j}u = \partial^2_{\mathbf{q}_i\mathbf{q}_j}u = \partial^{2,h}_{\mathbf{q}_i\mathbf{q}_j}u_h$ vanish because of the principle of the spectral decomposition (cf. sections 3 and 4.2). Conversely, for real applications the approximations $D^{2,h}u_h \approx D^2u$ and $\mathbf{p}_{i,T}\approx\mathbf{q}_i(x)$ have to be good enough. Additionally the element T has to be small enough such that $\partial^2_{\mathbf{p}_i\mathbf{p}_j}u$ does not change too much and, in particular, remains neglectable compared to $\partial^2_{\mathbf{p}_i\mathbf{p}_i}u$.

Assumption (A.3): $h_{i,T}^2 \cdot \|\partial^2_{\mathbf{p}_i\mathbf{p}_i} u\|_T \sim \alpha_{\mathcal{T}}^2 \cdot |T|^{1/2} \qquad i = 1,2,3, \quad \forall\, T \in \mathcal{T}$

To show the plausibility of the assumption,

(a) we evaluate $\|\partial^2_{\mathbf{p}_i\mathbf{p}_i} u\|_{T_{new}}$ by some numerical integration rule,
(b) we assume $h_{i,T_{new}} \approx H_i(x)$ and $\mathbf{p}_{i,T_{new}} \approx \mathbf{q}_i(x)$ for some/all $x \in T_{new}$,
(c) we employ $D^{2,h}u_h \approx D^2 u$,
(d) and we utilize the definition (6) of $H_i(x)$.

To be precise, let a numerical integration scheme (on T_{new}) be given by some points $x_k \in T_{new}$ together with weights β_k. Then[4]

$$\begin{aligned}
h_{i,T_{new}}^4 \cdot \|\partial^2_{\mathbf{p}_i\mathbf{p}_i} u\|^2_{T_{new}} &\overset{(a)}{\approx} h_{i,T_{new}}^4 \cdot |T_{new}| \cdot \sum_{x_k} \beta_k \cdot (\partial^2_{\mathbf{p}_i\mathbf{p}_i} u(x_k))^2 \\
&\overset{(b)}{\approx} |T_{new}| \cdot \sum_{x_k} \beta_k \cdot H_i^4(x_k) \cdot (\partial^2_{\mathbf{q}_i\mathbf{q}_i} u(x_k))^2 \\
&\overset{(c)}{\approx} |T_{new}| \cdot \sum_{x_k} \beta_k \cdot H_i^4(x_k) \cdot (\partial^{2,h}_{\mathbf{q}_i\mathbf{q}_i} u_h(x_k))^2 \\
&\overset{(6)}{=} |T_{new}| \cdot \sum_{x_k} \beta_k \cdot \alpha_{\mathcal{T}}^4 \quad = \quad |T_{new}| \cdot \alpha_{\mathcal{T}}^4 \qquad .
\end{aligned}$$

If one increases the number of integration points then

- the integration rule is likely to improve in quality,
- but the approximations $h_{i,T_{new}} \approx H_i(x)$, $\mathbf{p}_{i,T_{new}} \approx \mathbf{q}_i(x)$ and $D^{2,h}u_h \approx D^2 u$ have to be accurate for more points, and are more critical to obtain.

Ultimately one can even use exact integration on the cost that the aforementioned equivalences have to hold for almost all $x \in T_{new}$:

$$\begin{aligned}
h_{i,T_{new}}^4 \cdot \|\partial^2_{\mathbf{p}_i\mathbf{p}_i} u\|^2_{T_{new}} &= h_{i,T_{new}}^4 \cdot \int_{T_{new}} (\partial^2_{\mathbf{p}_i\mathbf{p}_i} u(x))^2 \\
&\overset{(b)}{\approx} \int_{T_{new}} H_i^4(x) \cdot (\partial^2_{\mathbf{q}_i\mathbf{q}_i} u(x))^2 \\
&\overset{(c)}{\approx} \int_{T_{new}} H_i^4(x) \cdot (\partial^{2,h}_{\mathbf{q}_i\mathbf{q}_i} u_h(x))^2 \\
&\overset{(6)}{=} \int_{T_{new}} \alpha_{\mathcal{T}}^4 \;=\; |T_{new}| \cdot \alpha_{\mathcal{T}}^4 \qquad .
\end{aligned}$$

Since our demands on the integration rule and the equivalences can not be quantified in a more convenient way, we have chosen to present them in the form of assumption (A.3).

[4] The interesting case of a single point integration rule is of course contained.

Note, however, that the whole Hessian strategy (i.e. the choice of the stretching directions and lengths) plays a vital role in this condition, even if this is not immediately visible in the formula.

Summarizing the previous arguments, (A.3) can be expected to hold if $D^{2,h}u_h \approx D^2 u$ and $h_{i,T} \approx H_i(x)$, $\mathbf{p}_{i,T} \approx \mathbf{q}_i(x)$ for some/all $x \in T$. If some of these approximations are violated then the heuristic reasoning from above can not be applied. Nevertheless assumption (A.3) may still be valid since all three approximations interact in a rather complex way.

Assumption (A.4): $\|\partial_{\mathbf{p}_i}(u - \mathrm{I}_{CR}u)\|_T \gtrsim h_{i,T} \cdot \|\partial^2_{\mathbf{p}_i\mathbf{p}_i} u\|_T$

This property does not hold for arbitrary functions. Here we present a counterexample which employs a function that strongly oscillates over the element T.

Consider the triangle with vertices $(0,0)$, $(1,0)$, $(1,1)$ and the function $u(x_1,x_2) = \sin(2k\pi \cdot x_1)$. Then all edge integrals $\int_E u$ vanish giving the Crouzeix–Raviart interpolate $\mathrm{I}_{CR}u \equiv 0$. Straight–forward computations then yield

$$\|\partial_{x_1}(u - \mathrm{I}_{CR}u)\|_T \;=\; k \cdot \pi \qquad \text{and} \qquad \|\partial_{x_1x_1} u\|_T \;=\; k^2 \cdot 2\pi$$

and thus

$$\|\partial_{x_1}(u - \mathrm{I}_{CR}u)\|_T \;\not\gtrsim\; \|\partial_{x_1x_1} u\|_T \qquad \text{for } k \to \infty \qquad .$$

A transformation to the directional derivatives provides the actual counterexample[5]. A 3D counterexample can be constructed similarly.

Despite the example from above, assumption (A.4) can be expected to hold for sufficiently 'smooth' functions (e.g. without heavy oscillations). Further hopes are raised by the fact that eventually we do not require (A.4) itself. Instead the sum $\sum_{i=1}^3$ over all three directions, and the sum $\sum_{T\in\mathcal{T}}$ over all elements are the terms that matter. Thus some negative influence of a single triangle can hopefully be compensated (even if such cancelation effects can not be proven). An example of a weakened assumption is given in (A.4') on page 12.

Assumption (A.5): $m_1(u - u_h, \mathcal{T}) \sim m_1(u - \mathrm{I}_{CR}u, \mathcal{T})$

This assumption can be expected to hold if $u_h \approx \mathrm{I}_{CR}u$. Recall that the matching function m_1 emphasizes different directions to a different extend, i.e. the element–related numerator is

$$y_T \;=\; \sum_{i=1}^{3} \frac{h_{i,T}^2}{h_{min,T}^2} \cdot \|\partial_{\mathbf{p}_i}(u - \mathrm{I}_{CR}u)\|_T^2 \qquad ,$$

cf. the previous section. Hence the approximation $u_h \approx \mathrm{I}_{CR}u$ should be particularly good along the 'long' directions (represented by $h_{1,T}$ and probably $h_{2,T}$).

A slight modification of assumption (A.5) has also been investigated numerically. The examples of section 6 indicate that both terms of (A.5) differ by (usually much) less than 10%.

[5] The isotropic triangle here is of course a special case of an anisotropic element.

5 Derivation of the Hessian strategy in 2D

In the previous sections we have applied the Hessian strategy and have shown that then the matching function $m_1(u-u_h, \mathcal{T})$ is bounded. In this section we consider the problem in the reverse way: If m_1 is to be bounded, how do we have to choose the stretching direction and ratio? Since both items can not be chosen independently, the answer will be of the type: 'For a given stretching direction, the aspect ratio can be at most q_{max} for m_1 to be bounded'. It will turn out that this answer reproduces the Hessian strategy. Note that only the 2D case is considered.

We will start with some heuristic assumptions. Because of the general setting they are not formulated as stringent as before. First we replace u_h by the interpolant $\mathrm{I}_{CR}u$ resulting in

$$m_1(u-u_h, \mathcal{T}) \;\approx\; m_1(u-\mathrm{I}_{CR}u, \mathcal{T}) \qquad .$$

Still the whole term is to difficult to deal with; hence consider only the element contributions and demand $y_T \lesssim z_T$, i.e.

$$h_{min,T}^{-2} \sum_{i=1}^{2} h_{i,T}^2 \cdot \|\partial_{\mathbf{p}_i}(u-\mathrm{I}_{CR}u)\|_T^2 \;\lesssim\; \sum_{i=1}^{2} \|\partial_{\mathbf{p}_i}(u-\mathrm{I}_{CR}u)\|_T^2 \qquad ,$$

cf. (12)–(14). Recall that $h_{1,T} \geq h_{2,T}$ are the lengths of the triangle along the two orthogonal directions $\mathbf{p}_{1,T}$ and $\mathbf{p}_{2,T}$. Next the interpolation estimate (8) is applied. We (heuristically) assume that (8) is *sharp*, i.e. we assume

$$\|\partial_{\mathbf{p}_i}(u-\mathrm{I}_{CR}u)\|_T \sim \sum_{j=1}^{3} h_{j,T} \cdot \|\partial^2_{\mathbf{p}_i\mathbf{p}_j} u\|_T \qquad i=1,2,3.$$

Hence the following inequality should be satisfied

$$\begin{aligned} & \frac{h_{1,T}^4}{h_{2,T}^2} \cdot \|\partial^2_{\mathbf{p}_1\mathbf{p}_1} u\|_T^2 \;+\; h_{1,T}^2 \cdot \|\partial^2_{\mathbf{p}_1\mathbf{p}_2} u\|_T^2 \;+\; h_{2,T}^2 \cdot \|\partial^2_{\mathbf{p}_2\mathbf{p}_2} u\|_T^2 \;\lesssim \\ \lesssim\; & h_{1,T}^2 \cdot \|\partial^2_{\mathbf{p}_1\mathbf{p}_1} u\|_T^2 \;+\; h_{1,T}^2 \cdot \|\partial^2_{\mathbf{p}_1\mathbf{p}_2} u\|_T^2 \;+\; h_{2,T}^2 \cdot \|\partial^2_{\mathbf{p}_2\mathbf{p}_2} u\|_T^2 \end{aligned}$$

which holds (up to some constant factor) iff

$$\frac{h_{1,T}^4}{h_{2,T}^2} \cdot \|\partial^2_{\mathbf{p}_1\mathbf{p}_1} u\|_T^2 \;\lesssim\; h_{1,T}^2 \cdot \|\partial^2_{\mathbf{p}_1\mathbf{p}_2} u\|_T^2 \;+\; h_{2,T}^2 \cdot \|\partial^2_{\mathbf{p}_2\mathbf{p}_2} u\|_T^2$$

or, equivalently,

$$f \;:=\; \frac{q^2 \cdot \|\partial^2_{\mathbf{p}_1\mathbf{p}_1} u\|_T^2}{q \cdot \|\partial^2_{\mathbf{p}_1\mathbf{p}_2} u\|_T^2 \;+\; \|\partial^2_{\mathbf{p}_2\mathbf{p}_2} u\|_T^2} \;\lesssim\; 1 \tag{15}$$

$$\text{with} \qquad q \;:=\; h_{1,T}^2/h_{2,T}^2 \;>1 \qquad . \tag{16}$$

We want to express $\partial^2_{\mathbf{p}_i\mathbf{p}_j} u$ by means of D^2u, and thus start with the spectral decomposition (i.e. principal axes transformation) of $D^2u(x_0, y_0)$ at some point (x_0, y_0) of the element[6]. Hence $D^2u(x_0, y_0)$ is transformed into a diagonal matrix; that is, there are two orthogonal directions $\hat{x}, \hat{y}$ (which are the principal axes) such that the mixed directional derivative vanishes, $\partial^2_{\hat{x}\hat{y}} u(x_0, y_0) \equiv \partial_{\hat{x}} \partial_{\hat{y}} u(x_0, y_0) = 0$

Let the triangle T be rotated by an angle φ against the principal directions $(\hat{x}, \hat{y})$, i.e. $\varphi = \sphericalangle(\mathbf{p}_{1,T}, \hat{x})$. Set $c := \cos\varphi$, $s := \sin\varphi$, and let

$$P := \begin{bmatrix} c & s \\ -s & c \end{bmatrix}$$

be the usual rotation matrix. Then

$$\begin{bmatrix} \partial^2_{\mathbf{p}_1\mathbf{p}_1} u & \partial^2_{\mathbf{p}_1\mathbf{p}_2} u \\ \partial^2_{\mathbf{p}_2\mathbf{p}_1} u & \partial^2_{\mathbf{p}_2\mathbf{p}_2} u \end{bmatrix}(x,y) = P^\top \cdot \begin{bmatrix} \partial^2_{\hat{x}\hat{x}} u & \partial^2_{\hat{x}\hat{y}} u \\ \partial^2_{\hat{y}\hat{x}} u & \partial^2_{\hat{y}\hat{y}} u \end{bmatrix}(x,y) \cdot P$$

$$= \begin{bmatrix} c^2\partial^2_{\hat{x}\hat{x}} u - 2cs\partial^2_{\hat{x}\hat{y}} u + s^2\partial^2_{\hat{y}\hat{y}} u & cs\partial^2_{\hat{x}\hat{x}} u + (c^2 - s^2)\partial^2_{\hat{x}\hat{y}} u - cs\partial^2_{\hat{y}\hat{y}} u \\ cs\partial^2_{\hat{x}\hat{x}} u + (c^2 - s^2)\partial^2_{\hat{x}\hat{y}} u - cs\partial^2_{\hat{y}\hat{y}} u & s^2\partial^2_{\hat{x}\hat{x}} u + 2cs\partial^2_{\hat{x}\hat{y}} u + c^2\partial^2_{\hat{y}\hat{y}} u \end{bmatrix}(x,y) \quad .$$

Because of the spectral decomposition of $D^2u(x_0, y_0)$ one has $\partial^2_{\hat{x}\hat{y}} u(x_0, y_0) = 0$. However, $\partial^2_{\hat{x}\hat{y}} u$ is required not only at (x_0, y_0) but on all points $(x, y) \in T$. Hence we demand the important heuristic assumption that D^2u should not change too much across the triangle T. Thus $\partial^2_{\hat{x}\hat{y}} u(x, y)$ should be neglectable compared with $\partial^2_{\hat{x}\hat{x}} u(x, y)$ and $\partial^2_{\hat{y}\hat{y}} u(x, y)$ for $(x, y) \in T$. Furthermore we evaluate the norms $\| \cdot \|_T$ with a single point integration rule at (x_0, y_0). To be precise, we assume the equivalences

$$\begin{aligned} \|\partial^2_{\mathbf{p}_1\mathbf{p}_1} u\|^2_T &\sim |T| \cdot (c^2\partial^2_{\hat{x}\hat{x}} u + s^2\partial^2_{\hat{y}\hat{y}} u)^2(x_0, y_0) \\ \|\partial^2_{\mathbf{p}_1\mathbf{p}_2} u\|^2_T &\sim |T| \cdot (cs\partial^2_{\hat{x}\hat{x}} u - cs\partial^2_{\hat{y}\hat{y}} u)^2(x_0, y_0) \\ \|\partial^2_{\mathbf{p}_2\mathbf{p}_2} u\|^2_T &\sim |T| \cdot (s^2\partial^2_{\hat{x}\hat{x}} u + c^2\partial^2_{\hat{y}\hat{y}} u)^2(x_0, y_0) \quad . \end{aligned}$$

Inserting this into (15) yields

$$\begin{aligned} f = f(D^2u, q, \varphi) &= \frac{q^2 \cdot \|\partial^2_{\mathbf{p}_1\mathbf{p}_1} u\|^2_T}{q \cdot \|\partial^2_{\mathbf{p}_1\mathbf{p}_2} u\|^2_T + \|\partial^2_{\mathbf{p}_2\mathbf{p}_2} u\|^2_T} \\ &\sim \frac{q^2 \cdot (c^2\partial^2_{\hat{x}\hat{x}} u + s^2\partial^2_{\hat{y}\hat{y}} u)^2(x_0, y_0)}{q \cdot (cs\partial^2_{\hat{x}\hat{x}} u - cs\partial^2_{\hat{y}\hat{y}} u)^2(x_0, y_0) + (s^2\partial^2_{\hat{x}\hat{x}} u + c^2\partial^2_{\hat{y}\hat{y}} u)^2(x_0, y_0)} \\ &= \frac{q^2 \cdot (1 + t^2 \cdot \delta)^2}{q \cdot t^2(1 - \delta)^2 + (t^2 + \delta)^2} \\ &=: f(q, t, \delta) \end{aligned}$$

[6] For improved readability of this section we denote the coordinate system by (x, y) instead of (x_1, x_2).

with the abbreviations

$$t^2 := \frac{s^2}{c^2} = \tan^2\varphi \qquad\qquad \delta := \frac{\partial^2_{\hat{y}\hat{y}} u(x_0, y_0)}{\partial^2_{\hat{x}\hat{x}} u(x_0, y_0)} \quad . \tag{17}$$

According to (15) we aim at $f(q, t, \delta) \lesssim 1$, i.e.

$$q^2 \cdot (1 + t^2\,\delta)^2 \;\lesssim\; q \cdot t^2\,(1-\delta)^2 \;+\; (t^2+\delta)^2 \quad .$$

As already mentioned before, we want to obtain all q that satisfy this quadratic inequality for given t and δ. This leads to

$$1 \;<\; q \;\lesssim\; \frac{t^2(1-\delta)^2}{2(1+t^2\,\delta)^2} \;+\; \left[\frac{t^4(1-\delta)^4}{4(1+t^2\,\delta)^4} + \frac{(t^2+\delta)^2}{(1+t^2\delta)^2}\right]^{1/2}$$

and

$$q_{max} \;=\; q_{max}(t,\delta) \;\sim\; t^2\left(\frac{1-\delta}{1+t^2\,\delta}\right)^2 \;+\; \left|\frac{t^2+\delta}{1+t^2\,\delta}\right|$$

$$\max\frac{h_{1,T}}{h_{2,T}} \;=\; \sqrt{q_{max}} \;\sim\; |t| \cdot \left|\frac{1-\delta}{1+t^2\,\delta}\right| \;+\; \left|\frac{t^2+\delta}{1+t^2\,\delta}\right|^{1/2} \quad .$$

Keeping the heuristic assumptions and their limitations in mind, this equivalence describes the maximum aspect ratio such that the matching function m_1 is bounded. The maximum aspect ratios are given in dependence of

- the angle φ between the directions $\mathbf{p}_{i,T}$ of the triangle and the principal axes $\hat{x}, \hat{y}$,
- the ratio δ of the pure second order derivatives along the principal axes.

Let us now discuss the result for some distinctive cases where we prescribe δ and t and determine q_{max}. Without loss of generality assume that $|\delta| = |\partial^2_{\hat{y}\hat{y}} u(x_0, y_0)/\partial^2_{\hat{x}\hat{x}} u(x_0, y_0)| \geq 1$; otherwise we can mutually exchange the principal axes $\hat{x}$ for $\hat{y}$.

No.	Description	δ	$t = \tan\varphi$	$\max\frac{h_{1,T}}{h_{2,T}} = \sqrt{q_{max}}$
1	isotropic function	$\lvert\delta\rvert \sim 1$	arbitrary	$\sqrt{q_{max}} \sim 1$
2	anisotropic function	$\lvert\delta\rvert \gg 1$		
2a	– Hessian strategy mesh		$t = 0$	$\sqrt{q_{max}} \sim \lvert\delta\rvert^{1/2}$
2b	– small deviation from 'Hessian mesh'		$\lvert t\rvert \lesssim \lvert\delta\rvert^{-1/2}$	$\sqrt{q_{max}} \sim \lvert\delta\rvert^{1/2}$
2c	– strong deviation from 'Hessian mesh'		$\lvert t\rvert \sim 1$	$\sqrt{q_{max}} \sim 1$
2d	– completely wrong mesh		$\lvert t\rvert \gg 1$	$(\sqrt{q_{max}} \ll 1)$

We conclude that an *isotropic* function requires an *isotropic* mesh. For an *anisotropic* function, the Hessian strategy (case 2a) is reproduced: $\sqrt{q_{max}} \sim |\delta|^{1/2}$ is exactly the square root of the ratio of the eigenvalues of the Hessian, see (17). The same aspect ratio is possible

even if the triangle T is not exactly aligned with the principal directions (case 2b). The deviation (i.e. the angle between the principal directions and T) can be up to

$$\varphi \approx \tan\varphi = t \sim |\delta|^{-1/2} \sim 1/\sqrt{q_{max}} \sim h_{2,T}/h_{1,T} \qquad .$$

It is probably surprising that the same angle of the deviation occurs in [AD92, Theorem 2] when investigating interpolation estimates there.

If the elements show a large deviation from the principal axes (case 2c) then only an isotropic mesh is possible.

The last (rather hypothetic) case 2d considers a completely wrong mesh, i.e. the triangle T is rotated by about 90^{O} against the principal directions (corresponding to $t = \tan\varphi \gg 1$). Hence the 'long' direction $\mathbf{p}_{1,T}$ corresponds to the 'large' derivative $\partial^2_{\hat{y}\hat{y}} u$, and the stretching is thus the opposite way. Then we obtain a contradiction to $q > 1$; therefore the matching function m_1 will be unbounded here.

6 Numerical experiments

In this section we will numerically explore whether assumption (A.5) is a realistic demand. For implementation reasons we consider the Lagrange interpolate I_{L} instead of I_{CR}, i.e. we investigate whether

$$m_1(u - u_h, \mathcal{T}) \;\sim\; m_1(u - \mathrm{I}_{L} u, \mathcal{T}) \qquad \text{(A.5')}$$

holds. In forthcoming software developments the Crouzeix–Raviart interpolate I_{CR} will be incorporated as well. It is strongly to be expected that the results for I_{L} carry over to I_{CR}.

Note that we do not apply the Hessian strategy here; instead we utilize meshes that were constructed on *a priori* knowledge.

6.1 Example 1

When solving a Poisson problem in three-dimensional domains Ω, a typical occurrence of an anisotropic solution is induced by an edge with an angle $\omega > \pi$, and/or by a change of the boundary conditions, cf. also [Kun99a] and the citations therein. Therefore we choose the following test problem which has already been discussed in [Kun99a, Ape97] (partly in a slightly different form). Solve the three-dimensional Poisson problem

$$-\Delta u \;=\; f \quad \text{in } \Omega \qquad , \qquad u \;=\; u_0 \quad \text{on } \Gamma_D \qquad , \qquad \partial u/\partial n \;=\; g_N \quad \text{on } \Gamma_N \qquad .$$

The domain Ω consists of three quarters of a cylinder, i.e.

$$\Omega = \{(r\cos\varphi\,,\, r\sin\varphi\,,\, z) \in \mathbb{R}^3 \quad : \; 0 < r, z < 1\,,\, 0 < \varphi < 3\pi/2\} \qquad ,$$

cf. also figure 2. The Neumann boundary Γ_N shall consist of the top and bottom plane of Ω, and of the plane described by $x = 0$. Let the Dirichlet boundary be $\Gamma_D := \partial\Omega \setminus \Gamma_N$.

The exact solution u (in cylindrical coordinates) is prescribed to be

$$\begin{aligned} u(r,\varphi,z) &:= r^\lambda \cdot \sin(\lambda\varphi) \cdot (1+\gamma(z)) \qquad \text{with } \lambda = 1/3 \\ \text{and} \qquad \gamma(z) &:= \begin{cases} (2z-1)\cdot 2z & \text{when } z \in [0,1/2] \\ (2z-1)\cdot(3-4z) & \text{when } z \in (1/2,1] \end{cases} \quad . \end{aligned}$$

The corresponding right-hand side $f = -\Delta u$ is in $L_p(\Omega)$ for all $p \in [1,\infty]$, but it has a jump at $z = 1/2$. The boundary conditions u_0 and g_N are chosen according to u. The exact solution u displays an edge singularity of the type r^λ. This implies an anisotropy of u along the z-axis.

The sequence of meshes is constructed as follows. First, the domain Ω is *isotropically* and quasi-uniformly meshed, with $h \sim 2^{-k}$, $k = 0, 1, 2 \ldots$ (note that the curved boundary is approximated). The final, *anisotropic* mesh is obtained by the subsequent nodal coordinate transformation (also known as mesh grading)

$$\begin{pmatrix} \eta \\ \xi \end{pmatrix} \longrightarrow \begin{pmatrix} x \\ y \end{pmatrix} := \hat{r}^{\frac{1}{\mu}-1} \cdot \begin{pmatrix} \eta \\ \xi \end{pmatrix} \qquad \text{with } \hat{r} = \sqrt{\eta^2+\xi^2} \quad . \tag{18}$$

This ensures the adaption of the mesh to u. The grading parameter μ is chosen to be $\mu = 0.3$ resulting in an optimal rate of convergence in the energy norm, i.e. $|||u - u_h||| \sim N^{-1/3}$, with N being the degrees of freedom [Ape97]. The corresponding meshes before and after the mesh grading are depicted in figure 2.

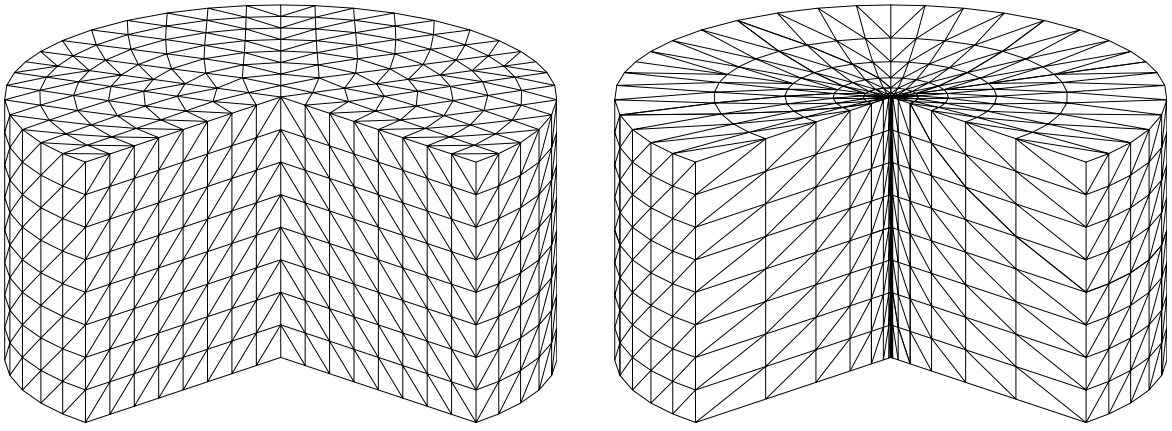

Figure 2: Mesh 1d before and after mesh grading

The values of the matching functions $m_1(u-u_h, \mathcal{T})$ and $m_1(u-\mathrm{I}_L u, \mathcal{T})$ are given below, together with some mesh information.

	# Elements	Max. aspect ratio	$m_1(u-u_h,\mathcal{T})$	$m_1(u-\mathrm{I}_L u,\mathcal{T})$
Mesh 1a	12	2.2	1.63	1.63
Mesh 1b	96	9.7	2.26	2.14
Mesh 1c	768	30.6	2.18	2.03
Mesh 1d	6 144	154.0	2.10	2.02
Mesh 1e	49 152	775.8	2.06	2.02
Mesh 1f	393 216	3 910.0	2.06	2.03
Mesh 1g	3 145 728	19 705.1	2.06	2.04

One observes that replacing u_h by $\mathrm{I}_L u$ in the matching function changes the value only slightly. Thus assumption (A.5') is valid here, and (A.5) is expected to hold as well.

Furthermore the small values of $m_1(u-u_h,\mathcal{T})$ indicate that the anisotropic meshes utilized are really suitable for this kind of problem.

6.2 Example 2

The second example is a singularly perturbed reaction diffusion model problem that has already been analysed in [KV99].

$$-\varepsilon\Delta u + u = 0 \quad \text{in } \Omega := [0,1]^3 \qquad , \qquad u = u_0 \quad \text{on } \Gamma_D := \partial\Omega$$

with the perturbation parameter $\varepsilon = 10^{-4}$. The exact solution is prescribed to be

$$u = e^{-x/\sqrt{\varepsilon}} + e^{-y/\sqrt{\varepsilon}} + e^{-z/\sqrt{\varepsilon}} \qquad .$$

It displays typical boundary layers along the planes $x = 0$, $y = 0$, and $z = 0$. The boundary value u_0 is chosen accordingly.

The domain is discretized by a sequence of meshes, each one being the tensor product of three one–dimensional Bakhvalov–like meshes [Bak69] with 2^k intervals in [0,1], $k = 1 \ldots 6$. To describe the 1D nodal distribution properly, denote the transition point of the boundary layer by $\tau := \sqrt{\varepsilon}|\ln\sqrt{\varepsilon}|$. Then 2^{k-1} nodes are *exponentially* distributed in the boundary layer interval $[0,\tau]$ whereas the remaining interval $[\tau,1]$ is divided into 2^{k-1} *equidistant* intervals, cf. figure 3. More precisely, the (1D) nodal coordinate of the m-th node is

$$x_m := \begin{cases} -\beta\sqrt{\varepsilon}\ln\left[1 - \dfrac{m}{2^{k-1}}(1 - e^{-\tau/\beta/\sqrt{\varepsilon}})\right] & \text{for } m = 0 \ldots 2^{k-1}, \beta = 3/2 \\ \tau + (1-\tau)\cdot\left(\dfrac{m}{2^{k-1}} - 1\right) & \text{for } m = 2^{k-1}+1 \ldots 2^k \end{cases} .$$

Note that the only difference to the original Bakhvalov mesh consists in the slightly different choice of the transition point τ.

Again the values of the matching functions $m_1(u-u_h,\mathcal{T})$ and $m_1(u-\mathrm{I}_L u,\mathcal{T})$, and some mesh information are given below.

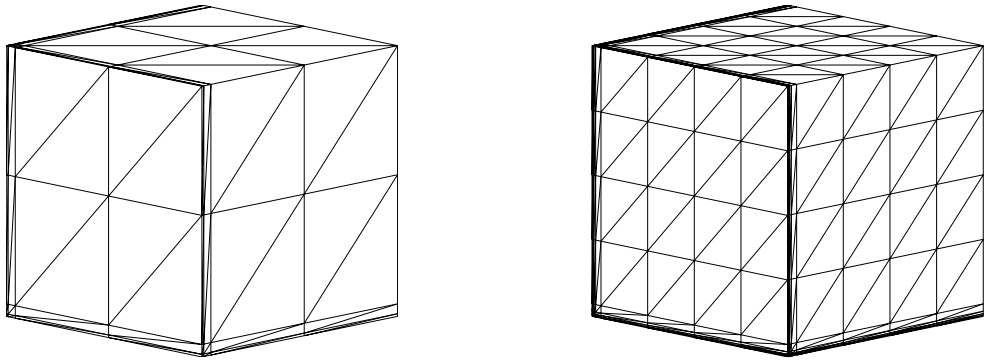

Figure 3: Mesh 2b – Mesh 2c

	# Elements	Max. aspect ratio	$m_1(u-u_h,\mathcal{T})$	$m_1(u-\mathrm{I}_L u,\mathcal{T})$
Mesh 2a	48	29.4	1.55	1.55
Mesh 2b	384	69.5	1.62	1.61
Mesh 2c	3 072	82.6	1.69	1.67
Mesh 2d	24 576	88.6	1.88	1.86
Mesh 2e	196 608	91.5	2.37	2.36
Mesh 2f	1 572 864	92.9	3.04	3.04

The table shows an astonishing coincidence of both matching functions. Therefore here u_h can be replaced by $\mathrm{I}_L u$ without changing the values much, and assumption (A.5') is clearly valid.

7 Summary

In an anisotropic adaptive algorithm it is a common desire to have an error estimator that provides the error size but also the optimal stretching directions and stretching ratio of the underlying anisotropic mesh. Since the last two information can not yet be extracted (for any of the known estimators), we have investigated the so–called Hessian strategy which provides exactly these information, based on some heuristic assumptions.

Our main result proves that an anisotropic mesh constructed by the Hessian strategy implies a bounded matching function, i.e. $m_1(u-u_h,\mathcal{T}) \lesssim 1$. Consequently reliable and efficient error estimation is possible. In the 2D case it is even possible to derive the Hessian strategy directly from the condition $m_1(u-u_h,\mathcal{T}) \lesssim 1$.

Because of the heuristic nature of the Hessian strategy we too require some heuristic assumptions. Nevertheless they are presented as precise as possible, and in a rather general form such that other meshing strategies can (hopefully) be analysed as well.

Altogether this work provides further inside into the nature of anisotropic error estimation, and the matching function in particular.

References

[AD92] Th. Apel and M. Dobrowolski. Anisotropic interpolation with applications to the finite element method. *Computing*, 47:277–293, 1992.

[ANS99] Th. Apel, S. Nicaise, and J. Schöberl. Crouzeix-raviart type finite elements on anisotropic meshes. Preprint SFB393/99-10, TU Chemnitz, 1999.

[Ape97] Th. Apel. Interpolation of non-smooth functions on anisotropic finite element meshes. Preprint SFB393/97-6, TU Chemnitz, 1997. To appear in Math. Modeling Numer. Anal.

[Bak69] N. S. Bakhvalov. Optimization of methods for the solution of boundary value problems in the presence of a boundary layer. *Zh. Vychisl. Mat. i Mat. Fiz.*, 9:841–859, 1969. In Russian.

[BH96] F. J. Bossen and P. S. Heckbert. A pliant method for anisotropic mesh generation. In *Proceedings of the* 5^{th} *Annual International Meshing Roundtable*, Pittsburgh, PA, 1996. Sandia National Laboratories.

[BK94] R. Beinert and D. Kröner. Finite volume methods with local mesh alignment in 2–D. In *Adaptive Methods – Algorithms, Theory and Applications*, volume 46 of *Notes on Num. Fluid Mechanics*, pages 38–53, Braunschweig, 1994. Vieweg.

[CHM95] M. J. Castro-Díaz, F. Hecht, and B. Mohammadi. New progress in anisotropic grid adaption for inviscid and viscous flow simulations. In *Proceedings of the* 4^{th} *Annual International Meshing Roundtable*, pages 73–85, Albuquerque, NM, 1995. Sandia National Laboratories. Also Report 2671 at INRIA.

[DGP99] M. Dobrowolski, S. Gräf, and C. Pflaum. On a posteriori error estimators in the finite element method on anisotropic meshes. *Electronic Transactions Num. Anal.*, 8:36–45, 1999.

[Dör96] W. Dörfler. A convergent adaptive algorithm for Poisson's equation. *SIAM J. Num. Anal.*, 33:1106–1124, 1996.

[FLR96] J. Fröhlich, J. Lang, and R. Roitzsch. Selfadaptive finite element computations with smooth time controller and anisotropic refinement. Report 96–16, ZIB, 1996.

[KR90] R. Kornhuber and R. Roitzsch. On adaptive grid refinement in the presence of internal and boundary layers. *IMPACT of Computing in Sci. and Engrg.*, 2:40–72, 1990.

[Kun99a] G. Kunert. *A posteriori error estimation for anisotropic tetrahedral and triangular finite element meshes.* Logos Verlag, Berlin, 1999. Also PhD thesis, TU Chemnitz, http://www.tu-chemnitz.de/pub/1999/0012/index.html.

[Kun99b] G. Kunert. An a posteriori residual error estimator for the finite element method on anisotropic tetrahedral meshes. *to appear in Numer. Math.*, 1999.

[KV99] G. Kunert and R. Verfürth. Edge residuals dominate a posteriori error estimates for linear finite element methods on anisotropic triangular and tetrahedral meshes. *to appear in Numer. Math.*, 1999.

[MNS99] P. Morin, R. H. Nochetto, and K. G. Siebert. Data oscillation and convergence of adaptive fem. Report 17/1999, University of Freiburg, July 1999.

[Noc95] R. H. Nochetto. Pointwise a posteriori error estimators for elliptic problems on highly graded meshes. *Math. Comp.*, 64:1–22, 1995.

[PVMZ87] J. Peraire, M. Vahdati, K. Morgan, and O. C. Zienkiewicz. Adaptive remeshing for compressible flow computation. *J. Comp. Phys.*, 72:449–466, 1987.

[Rac93] W. Rachowicz. An anisotropic h–type mesh refinement strategy. *Comput. Methods Appl. Mech. Engrg.*, 109:169–181, 1993.

[RGK93] W. Rick, H. Greza, and W. Koschel. FCT-solution on adapted unstructured meshes for compressible high speed flow computations. In E. H. Hirschel, editor, *Flow simulation with high-performance computers I*, volume 38 of *Notes on Num. Fluid Mechanics*, pages 334–438. Vieweg, 1993.

[Sie96] K. G. Siebert. An a posteriori error estimator for anisotropic refinement. *Numer. Math.*, 73(3):373–398, 1996.

[Sim94] R. B. Simpson. Anisotropic mesh transformation and optimal error control. *Appl. Numer. Math.*, 14:183–198, 1994.

[VH96] R. Vilsmeier and D. Hänel. Computational aspects of flow simulation in three dimensional, unstructured, adaptive grids. In E. H. Hirschel, editor, *Flow simulation with high-performance computers II*, volume 52 of *Notes on Num. Fluid Mechanics*, pages 431–446. Vieweg, 1996.

[ZW94] O. C. Zienkiewicz and J. Wu. Automatic directional refinement in adaptive analysis of compressible flows. *Internat. J. Numer. Methods Engrg.*, 37:2189–2210, 1994.